Malaver Rojas, Jairo, Gonzalez, Felipe, Motta, Nunzio, & Villa, Tommaso Francesco
(2015)
Design and flight testing of an integrated solar powered UAV and WSN for remote gas sensing.
In Mattingly, R (Ed.) *Proceedings of the 2015 IEEE Aerospace Conference.*
Institute of Electrical and Electronics Engineers Inc., United States of America, pp. 1-10.

https://doi.org/10.1109/AERO.2015.7119209

Design and Flight Testing of an Integrated Solar Powered UAV and WSN for Remote Gas Sensing

Alexander Jairo Rojas Malaver
School of Chemistry, Physics and Mechanical Engineering (CPME)
Queensland University of Technology
2 George St, Brisbane QLD 4000
+61 31385106
Alexander.malaverrojas@qut.edu.au

Luis Felipe Gonzalez
Australian Research Centre for Aerospace Automation (ARCAA)
Queensland University of Technology
2 George St, Brisbane QLD 4000
+61 7 3138 1363
Felipe.gonzalez@qut.edu.au

Nunzio Motta
School of Chemistry, Physics and Mechanical Engineering (CPME)
Queensland University of Technology
2 George St, Brisbane QLD
+61 7 3138 5104
N.motta@qut.edu.au

Tommaso Francesco Villa
School of Chemistry, Physics and Mechanical Engineering (CPME)
Queensland University of Technology
2 George St, Brisbane QLD 4000
+61 31389084
TF.Villa@hdr.qut.edu.au

Abstract— **This paper describes a generic and integrated solar powered remote Unmanned Air Vehicles (UAV) and Wireless Sensor Network (WSN) gas sensing system. The system uses a generic gas sensing system for CH_4 and CO_2 concentrations using metal oxide (MoX) and non-dispersive infrared sensors, and a new solar cell encapsulation method to power the UASs as well as a data management platform to store, analyse and share the information with operators and external users. The system was successfully field tested at ground and low altitudes, collecting, storing and transmitting data in real time to a central node for analysis and 3D mapping. The system can be used in a wide range of outdoor applications, especially in agriculture, bushfires, mining studies, opening the way to a ubiquitous low cost environmental monitoring. A video of the bench and flight test performed can be seen in the following link https://www.youtube.com/watch?v=Bwas7stYIxQ.**

TABLE OF CONTENTS

1. INTRODUCTION

UAVs are revolutionising remote environmental monitoring in environmental gas sensing due to their ability to carry instruments and sensors collecting data with high spatial and temporal resolution [2,30]. This paper discusses the development, integration, and flight testing of a gas sensing system installed on a UAV and a WSN. Figure 1 illustrates the concept developed.

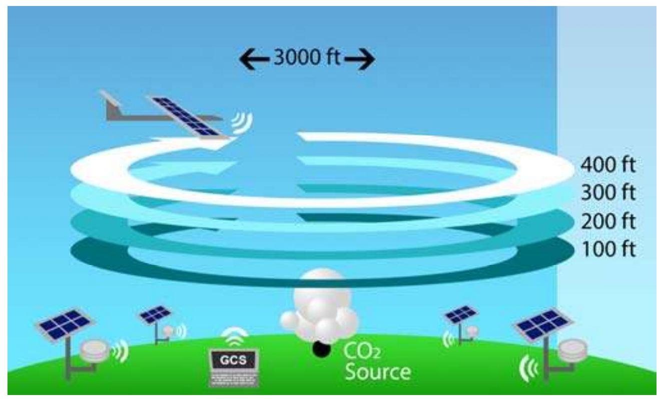

Figure 1 – Concept of a solar powered WSN and UAV gas sensing system.

UAVs have been used to sense environmental gases and are a powerful tool to reach remote areas and survey large regions. Optical gas sensing devices have been widely used among UAVs' users. Watai *et al.*[3] for instance discussed a non-dispersive infrared (NDIR) sensing system to monitor atmospheric CO_2 concentration onboard a small UAV, and designed an economic and accurate gas sensor system (± 0.26 *ppm* precision).The system performed several flight tests and achieved one hour flight autonomy with a 3.5 *kg* payload. McGonigle *et al.*[4] reported the first measurements of volcanic gases with a helicopter UAV at La Fossa crater, Volcano, Italy using an ultraviolet and infrared spectrometer to measure SO_2 and CO_2 gas concentrations. The UAV had 12 *min* flight autonomy, carrying a 3 *kg* payload. Astuti *et al.*[5, 6] developed a UAV for volcanic monitoring on Mt Etna using a fixed wing UAV to carry a CO_2 infrared spectrometer and a SO_2 electrochemical sensor. Saggiani *et al.*[7] in collaboration with the NASA Jet propulsion Laboratory flew the Raven UAV system above Stromboli volcano, Italy, in 2004. The UAV with a 3.5 *m* wingspan and maximum payload of 56 *kg* carried a visible and an IR camera and an experimental Fourier micro-interferometer based on MOEMS technology, to detect atmospheric trace gases. Berman *et al* [8] integrated a compact, lightweight atmospheric gas analyser onboard a mid-size SIERRA UAV with a 6.1 *m* wingspan and up to 40 *Kg* payload. Experimental tests were performed firstly at Crows Landing, CA, USA and subsequently in Salvbard Norway. In 2012 Khan *et al*.[9] stated that UAVs allowed for high spatial mapping of local greenhouse gas concentrations in the atmospheric boundary layer where land/atmosphere fluxes occur. The T-Rex Align 700E V2, a helicopter flew, with a main rotor diameter of 1.56 *m* and a flying mass excluding payload of approximately 4.7 *kg*. The UAV has a payload capacity up to 5 *kg* and flight time of 20 *m*. It was equipped with a very low power vertical cavity surface emitting lasers (VCSELs) to measure CO_2, CH_4 and H_2O.

The ability for a sensor node to communicate with others is an important tool to monitor large areas such as cities, roads and forests. Tracking and mapping gas plumes at ground level is one of the practical applications of WSNs. Therefore, WSNs has been used for environmental monitoring and monitoring of fugitive CH_4 emissions [10], coal fields or biomass degradation (landfills) [11], and NH_3 and N_2O gases released from fertilizer use [12, 13]. Although, this technology is already commercially available, the cost/benefit ratio is still high for extensive use. Metal Oxide (MoX) sensors and catalytic sensors are the preferred technology among WSNs' users based on current literature. MoXs have a large range of applications and have been employed in the detection of a wide variety of gases [14-16]. Recent advances in nanotechnology have benefited the development of MoX sensors as this technology facilitates the creation of gas sensors based on cutting edge materials to enhance detection performance [17]. Nano-scale materials can have significant differences from the physical, chemical, optical, mechanical, electronic and biological properties studied on the bulk sensor materials [17, 18]. At such as small size, the quantum regime becomes predominant and gives new properties beyond the classical limit. Morphology affects the performances of nano-structured sensors. Recently, more research has focused on 1-D nanostructures for gas sensing purposes due to high surface-to-volume ratio, quantum confinement and improved crystallinity [14]. The most common 1-D metal-oxide nanostructures used in the fabrication of gas sensors are in the form of nanorods, nanowires, nanofibers, nanotubes, nanobelts, nanoribbons, nanowhiskers, nanoneedles, nanopushpins, fibre-mats, urchin, lamellar and hierarchical dendrites [19]. MOX nanowires have demonstrated improved sensitivity to a wide range of gas species and stability due to their high degree of crystallinity

A major issue for WSN and UAV applications is power, as its availability limits service life, data collection and applications. WSN powered by solar energy has been developed and documented by several researchers [20, 21] [22, 23] with most designed for flight endurance [22]. This research focuses on the ability to fly the UAV while surveying the atmosphere by using solar energy. The rest of the paper is organized as follows: section 2 discuses Solar Powered Wireless Sensor Network (WSN) Subsystem, section 4 describes the solar powered UAV, section 4 discuses WSN and UAV field tests, and section 5 presents conclusions and future work.

2. SOLAR POWERED WIRELESS SENSORS NETWORK (WSN) SUBSYSTEM

Malaver *et al* described a generic gas sensing system and its application to WSN [24], developed as part of a collaborative research project between Brescia University (Italy) and QUT (Australia).This paper we extends the earlier work by adapting the gas sensor system to be installed on a Solar Powered UAV. The four principal components of the gas sensor system are shown in Figure 2: a network board, a gas sensor and sensor board interface, a humidity sensor, a heat sensor and control and solar panel and power electronics. The network card acquires the signal from the gas sensors and is able to propagate the data throughout multiple wireless sensor nodes in order to reach the base node. The base node communicates the data to the field computer, data of which can be stored, displayed and shared on a live webpage.

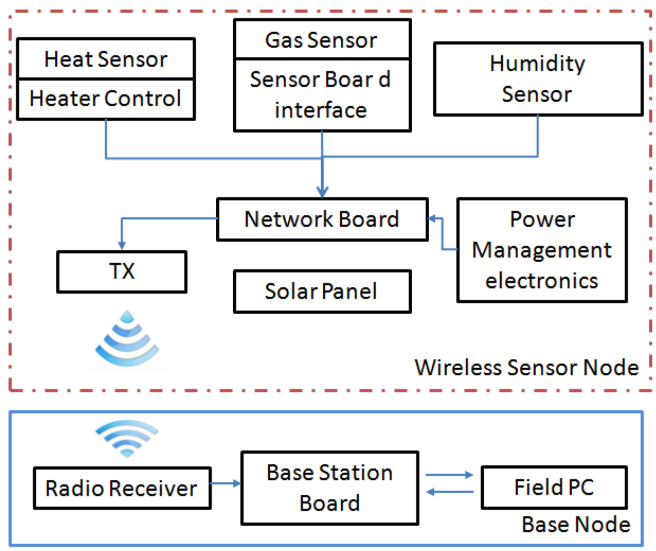

Figure 2 – Wireless gas sensing system node and base node configuration.

3. SOLAR POWERED UAV

The UAV has three main sub-systems that are integrated with the airframe in order to estimate gas concentration, navigate, and keep powered during operations. These sub-systems are depicted in Figure 3.

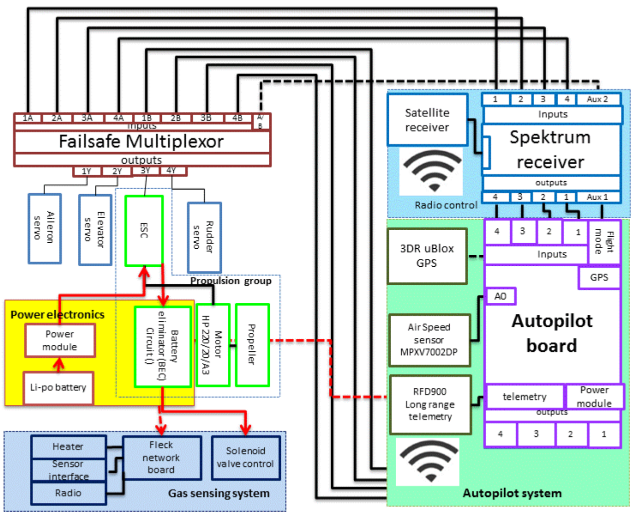

Figure 3 – General configuration of the UAV avionics integrated with the gas sensing system.

Gas Sensing System

The same gas sensing technology described in section 2 and used on the WSN was used for the UAV with some modifications to size, weight and power. Figure 4 illustrates these adaptations. The sample intake was adapted to allow the volume of gas volume for measurements. A fin shell was 3D printed to house the gas sensing system on top of the central wing. The fin shell was manufactured using lightweight materials (<50*g*) to avoid a significant increase in aircraft weight, which would reduce its performance. A small gas chamber (63 cm^3) was designed and installed inside the fin shell to retain the sample volume, while the sensor measures the gas concentration. The gas chamber has a T shape where the gas flows across the horizontal trajectory, with the sensor installed in the vertical cavity to ensure proper contact with the gas. A solenoid valve was also installed at the inlet of the chamber to control the time and flow of the sample intake. The closing time of the valve depends on the sensor response time because the sensor needs to stabilise before each measurement is taken. The opening time to flush the sample depends on the path-length of the valve, the chamber size and the aircraft speed. Opening the valve for 1*s* allows sufficient time to flush the pipeline and capture a new sample as the path-length of the chamber and solenoid is 10 *cm* (1 *cm*, maximum radius) and the average cruise speed of the UAS is 12 *m/s*. However, during bench and field testing the opening time of the valve was set to 2 *s* to ensure complete flush of the chamber, and closed for 5 *s* to determine gas concentration.

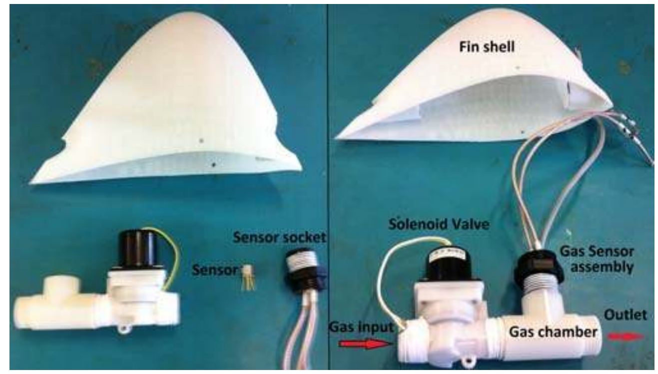

Figure 4 – Airborne gas sensing system: aerodynamic fin shell, gas sensor, sensor socket, gas chamber and solenoid valve.

The power for the gas sensing system is provided by an electronic battery eliminator circuit (BEC) that provides up to 5 *VDC,* 2 *A*. The 6 *V* required by the solenoid valve is provided by a step-up converter circuit attached to the BEC. Once the sensor board acquires the sensor signal, the information is transmitted to the base node using the radio module, antenna of which is installed on the top of the airframe.

UAV and Navigation System

The UAS developed in this work was based on the Green Falcon UAV[25]. The UAV airframe is easy to transport for fast deployment and hand launched. It has a wingspan of 2.52 *m*, AR of 13, and fuselage length of 960 *mm*.

The main component of the navigation system is the autopilot, which is equipped with an air speed sensor, gyro sensor, accelerometer, magnetometer, barometric pressure, GPS, airspeed and fail safe system. The principal goal of this device is to navigate the aircraft by controlling the altitude, speed, and direction. The autopilot used for the UAS was the ArduPilot Mega 2.5, which is a complete open source autopilot system with a high benefit/cost ratio [26] and low weight (23 *g*). The autopilot system works mainly in three modes: (*i*) autonomous mode to fully perform unmanned mission by pre-programing waypoints from the ground control station (GCS); (*ii*) stabilised mode to assist a ground pilot in controlling and stabilising the flight of an aircraft where the pilot has partial control of the aircraft and when there is no pilot input the autopilot will maintain a level flight; (*iii*) and manual mode, which is useful to perform the pre-flight check as the autopilot acts as a pass-through for all RC commands and also allows the pilot to freely preform manual take-offs, manoeuvres and landings when the autopilot is not pre-programed to perform these tasks. In all modes, the autopilot is capable of transmitting important flight information such as roll, pitch, yaw, airspeed, GPS position and battery status to the GCS by using the telemetry module.

The GPS system used was a LEA-6 (UBlox), which consumes low power, is small and lightweight (16.8 *g*) it has an update rate up to 5 *Hz* and is ideal for UAV applications. When the GPS is connected to the autopilot the coordinates are transmitted to the GCS using the same telemetry module of the autopilot. The GPS connects directly to the autopilot GPS port, and uses the RX, TX, GND and 5 *V* connections.

The airspeed sensor was the MPXV7002, which is a small piezo-resistive transducer that provides a digital output. The sensor has a pressure range: -2 to 2 *kPa* , *a* 0.5 to 4.5 *V* output 5.0 % maximum error over 0°*C* to 85°*C* and a temperature compensated over -40°*C* to 125°*C*. The radio control was the DX8 model from Spektrum a well-known and reliable technology for radio control applications. The system has 8 Channels, DSM2/DSMX modulation, AR8000 receiver, compatible with AR6000/BR6000 receivers and 1, 2, 3 or 4 selectable modes. A failsafe multiplexer was also installed and integrated with the autopilot. The failsafe system makes the operation of an UAV safer by pre-programing the autopilot actions when an RC signal loss is detected. This system is equipped with a multiplexer board that will re-route any RC signal directly to the servos and ESC in the case of autopilot failure or flight preferences. The autopilot activates *Circle mode* if RC signal is lost for more than 1.5*s;* the autopilot will start to circle the area if there is a signal loss detected up to 20 *s* [27]. If the previous waiting period expires with no detection of RC signal, the *RLT mode* is activated, and the autopilot will attempt to return to lunch position[27]. The GCS can trigger the *RLT mode*, when the telemetry connection is lost for more than 20 *s*.

The telemetry module used was the RFD900, which works at 900*MHz*, is lightweight (50 *g*), small in size, has a large transmission range (>40 *km*), and requires about 1 *W* (+30 *dBm*) transmit power. The ground module uses a standard RX, TX, GND and 5 *V* connections, which facilitate communication with the GCS by using a FDI to USB cable.

Power Management and Solar Wing

The total energy demand of the UAV was calculated based on the power consumption of the avionics, motor and gas sensing system, plus the lost energy caused by the efficiency of electronics and avionics (equation 1).

$$E_{d\_total} = \frac{(E_{av} + E_{gss})}{\eta_{pe} * \eta_{av}} \quad \frac{(42.12\ Wh + 0.8\ Wh)}{0.86 \ \ *0.9} = 55.4W \qquad (1)$$

Where: *Wh*

$\eta_{pe} = 0.86$,

$\eta_{av} = 0.90, \text{Eav} = 42.12\ Wh, \quad \text{Egss} = 0.8Wh$

The total energy demand (E_{d_total}) of the UAV is 55.4 *Wh*, which needs to be supplied by the solar wing and battery.

The solar wing was constructed using small silicon solar cell (SSC) ribbons connected in serial and parallel configuration to achieve the voltage and current required. Each SSC ribbon has an area of 0.00375 m^2 and an average of 12 % efficiency. The maximum area for the solar panels is limited by the wing area (490 cm^2), ailerons, narrow ends, and the area allocated for the gas sensor system (53 cm^2). Careful analysis of the location and configuration of the solar panels lead to 70 SSC ribbons were distributed along the three parts of the wing by placing 19 units on each side wing (total 38), and 32 units in the middle, for a total of 70 SSC units (0.2625 m^2). The weight density of a single SSC ribbon with the tabbing wire installed is 0.53 kg/m^2. A flexible capsule with the shape of the wing was made to allocate the SSC panels, to avoid losses in aerodynamic performance and to withstand mechanical stress due to vibrations of the UAV while flying. The solar panels were encapsulated using a clear resin, which is flexible and totally transparent to avoid output power losses. Figure 5 shows the UAV with the solar wing in flight.

Figure 5 – Green Falcon UAV in flight.

The internal connections are in serial configuration to obtain the desired voltage of each panel. The side wing panels were connected in series to reach a V_{oc} of 19 *V*, which produced a current flow of 1.16 *A*. The middle wing panel is the main section, and consisted of 32 SSC ribbons in serial configuration to produce a V_{oc} of 16 *V*, and I_{sc} of 1.16 *A*. The right and the left wing panels in serial configuration were connected in parallel to the middle wing panel to produce a final V_{oc} and I_{sc} value between 16-19 *V*, 2 *A*, respectively.

Using the full irradiation of the sun at 1000 W/m^2, the maximum output power can be calculated as follows:

$$P_{max} = \frac{Area_{SSC_{panel}} * i_{sun} * \eta_{SSC}}{1m^2} \qquad (2)$$

$$\boldsymbol{P_{max}} = \frac{0.2625\boldsymbol{m}^2 * 1000\ \boldsymbol{W} * 0.12}{1\boldsymbol{m}^2} = 31.5\ \boldsymbol{W} \quad (2)$$

Where:

$$Area_{SSC\_panel} = Area_{SSC\_ribbon} * 70 units = 0.2625 m^2$$

According to the Australian Bureau of meteorology, the mean sunshine hours in Brisbane (QLD, Australia) are 7.4 *h* with a mean irradiance of 750 *Wh*. The expected average energy produced by the solar wing is therefore:

$$Energy_{SSC\ panel} = \frac{0.2625 m^2 * 750 Wh * 0.12}{1 m^2} = 23.625 Wh$$

When one of the SSC panels is shaded, broken or does not receive enough illumination, the panel performance is affected to the point of becoming a load for those panels connected in parallel, or an obstruction for panels connected in series. In response to this, a diode was installed at the output of each panel to avoid any losses in performance due to this effect.

The total wing weight is 1610 *g* which means that 650 *g* is due to the SSC panel and encapsulation mass.

A commercial battery that complements the solar panel to meet the energy demand of the aircraft is a 4 *cell*, 3.0 *Ah* lithium polymer battery, which provides a nominal energy output of 44.4 *Wh*. However, for safety reasons and technical limitations, only 80 % of the battery capacity (35.52 *Wh*) was taken into account.

The total energy available is therefore 59.14 *Wh*, which is enough energy to satisfy the demand of 55.4 *Wh*.

The electronic board used to manage the solar and battery power is based on the BQ 24650 EVB from Texas Instrument [28]. The board works as a Maximum Power Point Tracker (MPPT), battery charger, and power path manager. This chip is from the same family as used for the WSN nodes, with a battery charge/discharge efficiency of 86 %. The system is easy to setup, as the circuit board has only three ports; one for the solar power inlet, one for the lithium battery, and the output power to energise the UAV systems. The voltage needed to charge the battery is selected by configuring a set of resistors that provided a voltage reference to the chip in the battery charge circuit. The circuit board allows the selection of a target output voltage to make the solar panel work at the maximum power point (MPP). The output voltage targeted was 14.8 *V,* which is close to the MMP of the panels and matches the battery voltage.

Propulsion System and Total Aircraft System

The main components of the propulsion group of the aircraft are the electronics speed controller (ESC); the brushless motor; and the propeller. The ESC used was the Plush 40 *A*, which can provide up to 40 *A* to the motor with a smooth throttle response, integrated battery eliminator circuit (BEC, 5*V*/3*A*), small size, weights 33 *g*, and is compatible with lithium polymer batteries with 2 to 6 *cells*. The ESC regulates the power from the battery to run the avionics and gas sensing system simultaneously. In the case of an energy shortage, the ESC cuts the motor off and maintains a minimum power to allow the pilot manoeuver an emergency landing. The brushless motor used was the *Plettenberg* HP/220/20/A3 P6 SL 5:1. The propeller used was the CFK Prop Graupner 4325 with a diameter of 43 and 25 is the pitch (in centimetres). The propeller is lightweight (64 *g*) due to the carbon fibre content, a twill cloth laid diagonally on the blade for extreme torsional rigidity. The propeller is designed for a high performance rotor [29].

The weight distribution of the UAS with the sensing system installed is illustrated in Figure 6 which shows the breakdown for the CO_2 only, but similar results were obtained for the nano-sensor. The total weight of the UAS with the CO_2 system was 2573 *g,* and with the nano-sensor system 2615 *g*. It is clear from Figure 6 that the wing and fuselage were the heaviest parts in the UAV, while the CO_2 gas sensing system or the nano-sensor system represents only 12 % and 14 % of the total weight, respectively.

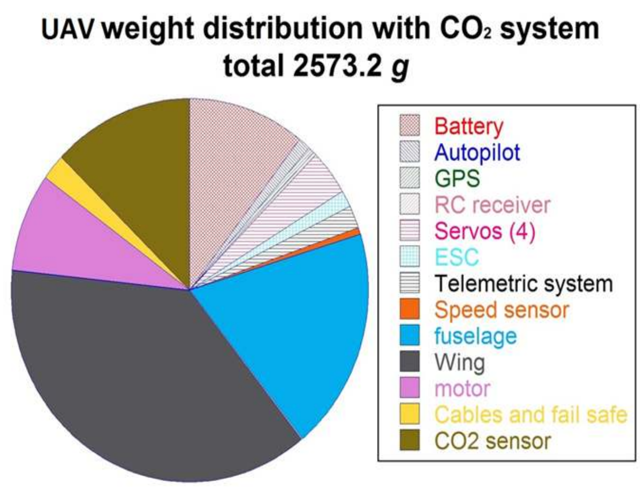

Figure 6 – Weight distribution of the Green Falcon UAV with CO_2 gas sensing system;

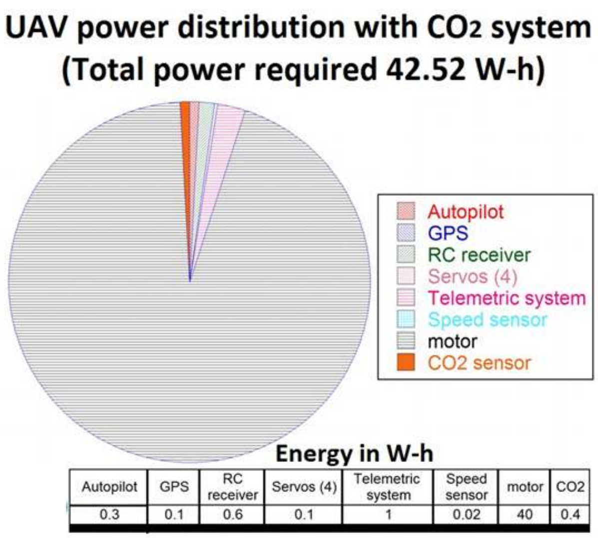

Figure 7 – Power consumption distribution of the UAV assembled with the CO_2 sensing system.

The power electronics had an average output voltage of 14.2 *V*, and the current intensity reached its maximum peak of about 6.5 *A* (consuming about 80 *W*), during take-off manoeuvres; however the average current consumption fluctuated between 1 *A* to 3 *A* (about 15 to 40 *W*), during regular flight operation. According to the GCS, the energy consumption of the UAV during the flight operation was in average 25 *Wh*, which is lower than the average energy measured in the bench test of about 40 *Wh*. The possible reason for this lower consumption is that the throttle of the motor was more active during the bench test than in the real flight operation, which is a positive feedback for the final design of the solar powered UAV for continuous flight during sun-light hours.

4. WSN AND UAV FIELD TEST

The target gas of the experiments was CO_2 due to the availability of the gas in the field testing area and the possibility of creating a contaminant source. Testing NO_2 and CH_4 in the field requires a different scenario that will be considered in future work. Only two of the four nodes developed for the WSN were tested as a proof of concept.

The complete system was tested at Christmas Creek, QLD, 23th July, 2013. The base station was located at the beginning of the airstrip, the pollutant source was located 30 *m* from the GCS, the CO_2 ground node and the weather station was deployed 20 *m* from the GCS, all south of the base node. The UAV mission was to fly in a circular trajectory up to an altitude of 50 *m* above ground level over the area monitored, above the sensor node and pollutant source. The CO_2 was released for 6 *min* at 0.0027 *kg/s* rate and average wind speed of 1.09 *m/s*.

The GCS was used to program the aircraft autopilot to perform a circular flight over the ground node and contaminant source for ten times in order to collect vast information about the contaminant concentration. The base node successfully received the transmissions from the ground and aerial node simultaneously. The aircraft showed a stable flight and the wing structure maintained its profile during flight; therefore, losses in aerodynamic performance are not expected. The power electronics successfully managed the energy from the solar wing and the battery ensuring power to the UAV during the whole flight. The overall performance of the aircraft indicates a successful construction technique of the solar wing integrated to the UAV.

CO_2 concentration values taken from ground and aerial nodes during the experiments are plotted in figure 8. The average CO_2 concentration registered by the ground node was 404 *ppm* during the first 164 *s*. Then, the average concentration increased slightly until it reached a peak of 442 *ppm* at the end of the experiment. The average CO_2 concentration registered by the aerial node was 400 *ppm*, with few CO_2 peaks above the average. The volume monitored by the UAV was 0.0012 km^3, based on the circular area travelled and flight altitude (~50 *m* AGL). The horizontal sampling resolution of the UAV was 88 *m/s* as the average cruise speed was 12.6 *m/s* and sampling frequency 7*s*. Vertical resolution of the samples was 10 *m* based on the uncertainty of the GPS and autopilot navigation.

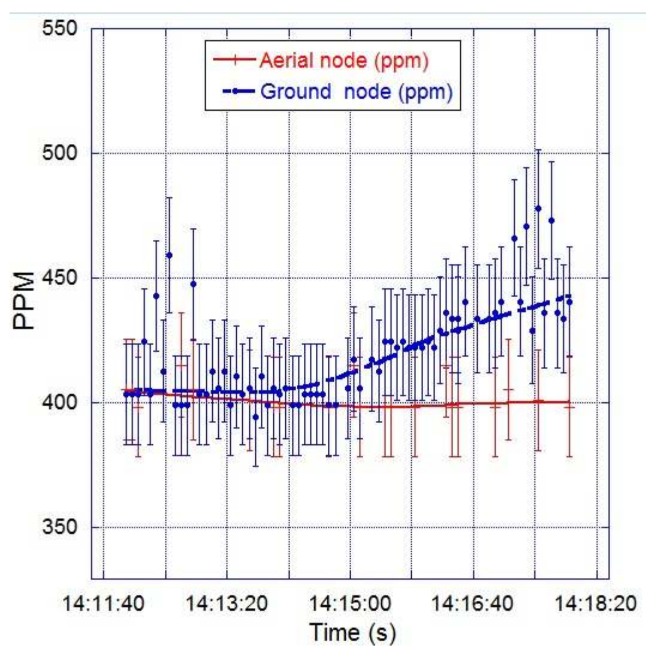

Figure 8 – CO_2 readings from the ground and aerial nodes during the experiment at Christmas Creek, QLD, Australia in 23/07/2013.

Figure 9 shows the UAV tracks during the experiment, the contaminant source origin and direction of the dispersion due to wind effect. The average wind speed was 1.5 *m/s,* mostly a in North-east direction.

Figure 9 – GPS tracks of the UAV during the mission, the source of contamination and the wind direction.

Figure 10 shows the latitude and longitude coordinates of each taken sample with their respective CO_2 concentration. The fact that the CO_2 readings from the UAV did not show significant variations indicates that the contaminant release rate and duration were not long enough to affect significantly a volume of 0.0012 km^3 within the time span of the experiment (6 *min*). In addition, the wind strength diluted the pollutant emissions to levels below the sensitivity of the equipment. Geo-location of the taken sample was possible by synchronising the logs of the network board and autopilot before the mission started. The ability to geo-locate the sample and register the time allows the reconstruction of the samples in three dimensions and facilitates the visualisation of local concentrations, analysis of their dynamics and correlations with variables such as temperature and pressure.

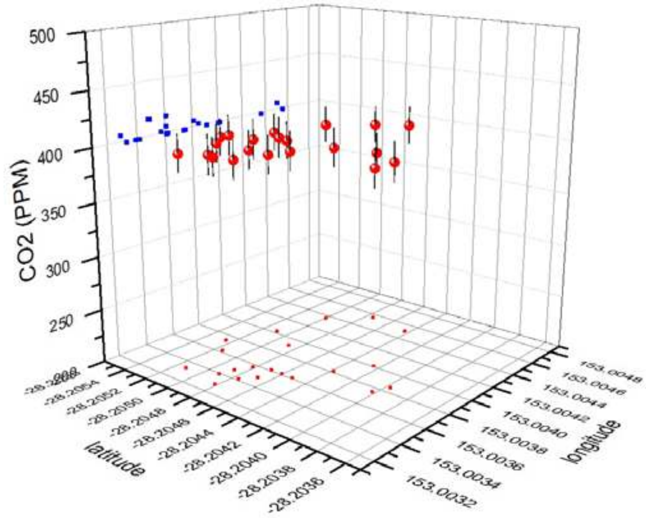

Figure 10 – Readings of the CO_2 gas sensing system on board Green Falcon UAV, showing the latitude, longitude and concentration of each sample.

5. CONCLUSIONS

This paper described a generic gas sensing and monitoring system of a solar powered WSN and UAV for environmental monitoring. The most meaningful results are described as follows:

A resistive gas sensing system and a NDIR module were created and adapted for aerial missions. The technology developed was successfully tested, showing reliable performance and meeting the payload constraints of a small UAV. MoX sensors were evaluated as a generic sensing platform for WSNs and UAVs. The results of the investigation and experiments showed that MoX sensors have appealing characteristics in view of the integration of WSN and UAV sensing. The reasons are the low energy consumption, lightness of the system, small dimensions, low computational resources demand, and inexpensive production. However, where fast sampling and high resolution (*ppb*) is required, optical sensing is the most suitable technology at the expense of weight and energy.

A small solar powered UAV was assembled, equipped with the gas sensing system, and successfully tested in the field. It is recommended for further experiments to increase the contaminant rate release and duration to produce significant CO_2 variation in the volume monitored by the UAV. Faster sampling frequency is also desirable, especially when the wind blows in a specific direction, which narrows the detection area.

A video of the extensive bench test performed for this work on the Green Falcon UAV can be seen in the following link https://www.youtube.com/watch?v=Bwas7stYIxQ.

Acknowledgement

The authors would like to acknowledge the financial support from the Queensland Government through the NIRAP project, "Solar powered Nano sensors", ARCAA for their technical support, Fazl Alabodi and Mandeep Saini as well as the support from Steven Bulmer the Green Falcon pilot.

6. References

[1] Hung, J. Y. and Gonzalez, L. F. On parallel hybrid-electric propulsion system for unmanned aerial vehicles. *Progress in Aerospace Sciences*, *51*, pp. 1-17, 2012.

[2] Borges de Sousa J., G.A.G., *Unmanned vehicles for environmental data collection.* Clean Techn Environ Policy, 13: p. 369–380, 2010.

[3] Watai, T. Machida, T. Ishizaki, N. Inoue, G. *A Lightweight Observation System for Atmospheric Carbon Dioxide Concentration Using a Small Unmanned Aerial Vehicle.* Journal of Atmospheric and Oceanic Technology, 23(5): p. 700-710, 2005.

[4] McGonigle, A. J. S. Giudice, G. Tamburello, A. Hodson, J. Gurrieri, S. *Unmanned aerial vehicle measurements of volcanic carbon dioxide fluxes.* Geophysical Research Letters, 35(6), 2008.

[5] Astuti, G. Giudice, G. Longo, D. Melita, C. D. Muscato G. Orlando A. *An Overview of the "Volcan Project": An UAS for Exploration of Volcanic Environments.* J. Intell. Robotics Syst. 54(1-3): p. 471-494, 2009.

[6] Astuti, G. Longo, D. Melita, C.D. Muscato, G. Orlando, A. *HIL tuning of UAV for exploration of risky environments.* International Journal of Advanced Robotic Systems, 5(4): p. 419-424, 2008.

[7] Saggiani, G. Persiani, F. Ceruti, A. Tortora, P. Troiani, E. Giuletti, F. Amici, S. Buongiorno, M. Distefano, G. Bentini, G. *A UAV system for observing volcanoes and natural hazards*. in *AGU Fall Meeting Abstracts*, 1: p. 5, 2007.

[8] Berman, E. S. F. Fladeland, M. Liem, J. Kolyer, R. Gupta, M. *Greenhouse gas analyzer for measurements of carbon dioxide, methane, and water vapor aboard an unmanned aerial vehicle.* Sensors and Actuators B-Chemical, 169: p. 128-135, 2012.

[9] Khan, A. Schaefer, D. Tao, L. Miller, D. J. Sun, K. Zondlo, M. A. Harrison, W. A. Roscoe, B. Lary, D. J. *Low Power Greenhouse Gas Sensors for Unmanned Aerial Vehicles.* Remote Sensing, 4(5): p. 1355-1368, 2012.

[10] Tümer, A. E. Gündüz, M. Design of a methane monitoring system based on wireless sensor networks. Scientific Research and Essays, 5: p. 799-805, 2010.

[11] Mitra, S. Duttagupta, S. P. Tuckley, K. Ekram, S. *Wireless Sensor Network Based Localization and Threat Estimation of Hazardous Landfill Gas Source*. IEEE International Conference on Industrial Technology. New York: IEEE. 349-355, 2012.

[12] Cho, J.H. Kim, Y.W. Na, K.J. Jeon, G.J., *Wireless electronic nose system for real-time quantitative analysis of gas mixtures using micro-gas sensor array and neuro-fuzzy network.* Sensors and Actuators B: Chemical, 134: p. 104 - 111, 2008.

[13] Ruiz-Garcia, L. Lunadei, L. Barreiro, P. Robla, I. *A Review of Wireless Sensor Technologies and Applications in Agriculture and Food Industry: State of the Art and Current Trends.* Sensors, 9: p. 4728-4750, 2009.

[14] Wang, C. Yin, L. Zhang, L. Xiang, D. Gao, R. *Metal Oxide Gas Sensors: Sensitivity and Influencing Factors.* Sensors, 10(3): p. 2088-2106, 2010.

[15] Sun, Y.F. Liu, S.B. Meng, F.L. Liu, J.Y. Jin, Z. Kong, L.T. Liu, J.H. *Metal Oxide Nanostructures and Their Gas Sensing Properties: A Review.* Sensors, 12(3): p. 2610-2631, 2012.

[16] Soldano, C. Comini, E. Baratto, C. Ferroni, M. Faglia, G. Sberveglieri, G. *Metal Oxides Mono-Dimensional Nanostructures for Gas Sensing and Light Emission.* Journal of the American Ceramic Society, 95(3): p. 831-850, 2012.

[17] Kalantar-zadeh, K. and Fry, B. *Nanotechnology-enabled sensors*. August 2008 ed. Anal Bioanal Chem. Springer-Verlag 2008.

[18] Cao, G. *Nanostructures and nanomaterials: Synthesis, properties and applications.* London: Imperial College Press, 2004.

[19] Arafat, M. M. Dinan, B. Akbar, Sheikh A. Haseeb, A. S. M. A. *Gas Sensors Based on One Dimensional Nanostructured Metal-Oxides: A Review.* Sensors, 12(6): p. 7207-7258, 2012.

[20] Win, K.K. Wu, X. Dasgupta, S. Wen, W.J. Kumar, R. Panda, S.K, *Efficient Solar Energy Harvester for Wireless Sensor Nodes.* IEEE, International Conference on Communication Systems (ICCS), p. 289-294, 2010.

[21] Alippi, C. Camplani, R. Galperti, C. Roveri, M. *A Robust, Adaptive, Solar-Powered WSN Framework for Aquatic Environmental Monitoring*. IEEE, Sensors, 11(1): p. 45-55, 2011.

[22] Noth, A. *History of Solar flight*. Autonomous Systems Lab, Swiss Federal Institute of Technology Zürich, 2008.

[23] Colella, N.J. and Wenneker, G. S. *Pathfinder. Developing a solar rechargeable aircraft.* Potentials, IEEE, 15(1): p. 18-23, 1996.

[24] Malaver Rojas, J.A. Motta, N. Corke, P. Bell, J. *Development of a gas nanosensor node powered by solar cells*. In *Solar2011, the 49th AuSES Annual Conference*, Australian Solar Energy Society, 2011.

[25] Malaver Rojas, J.A. Motta, N. Gonzalez, L. F. Corke, P. Depari, A. *Towards the development of a gas sensor system for monitoring pollutant gases in the low troposphere using small unmanned aerial vehicles.* Workshop on Robotics for Environmental Monitoring, 2012.

[26] *Ardupilot-mega*. 2013; Available from: https://code.google.com/p/ardupilot-mega/wiki/Introduction.

[27] *Failsafe autopilot funtion*. 2013; Available from: https://code.google.com/p/ardupilot-mega/wiki/APM2xFailsafe.

[28] *bq24650EVM Synchronous, Switch-Mode, Battery Charge Controller for Solar Power*, T. Instrument, Editor. 2010.

[29] *Propellers*. 2013; Available from: http://www.gravesrc.com/category_s/166.htm.

[30] Gonzalez, F., Castro, M. P. G.,Narayan, P., Walker, R., & Zeller,L. (2011). *Development of an autonomous unmannedaerial system to collect time-stamped samples from theatmosphere and localize potential pathogen sources*. Journal of Field Robotics, 28(6), 961–976.

BIOGRAPHY

Alexander Jairo Rojas Malaver *received his PhD form QUT, Brisbane-Australia in 2014. Alexander is interested in developing technology for environmental monitoring. He is a highly motivated engineer/scientist with extensive knowledge and experience in sensors, wireless communication, laboratory equipment, solar power applications, and unmanned aerial systems (UASs). He developed a solar UAS equipped with a nano-sensor system to monitor harmful gases affecting the environment. The UAS was integrated to a wireless sensor network on ground for an effective 3D monitoring. He is actively involved in research and teaching activities in QUT since 2011.*

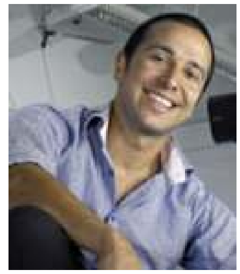

Luis Felipe Gonzalez *has a Ph.D. degree in multidisciplinary design optimization methods for unmanned aerial vehicle (UAV) systems from the University of Sydney, Sydney, Australia, in 2006. He is currently a Senior Lecturer with the Queensland University of Technology and the Australian Research Centre for Aerospace Automation (ARCAA), Brisbane, Australia. Felipe is the research lead for UAVs in environmental remotes sensing (precision agriculture, gas sensing ecology) at ARCAA. He has developed eight operational UAVs and has written 18 journal papers and more than 40 peer-reviewed papers on UAVs and remote sensing.*

Associate Professor **Nunzio Motta** *obtained his Laurea in Physics in 1981 (La Sapienza – Roma) and his PhD in Physics in 1986 (SNS - Pisa). He is internationally recognized in the field of material science, with over 25 year experience in growth and characterization of nanostructures. Since 2004, he is currently leading research at QUT in solar energy and environmental nanotechnology. Nunzio, chair of the NanoS-E3 conference since 2007, obtained several visiting positions in various research institutions across Europe, published more than 130 papers in material science and surface physics and has been leader in many international research projects in the area of nanotechnology. He is Associate editor of the Beilstein Journal of Nanotechnology, Advanced Device Materials and Nanomaterials and Nanotechnology.*

Tommaso Francesco Villa *has a MSc in Industrial Pharmacy (University of Milan – Milano, Italy) with a major in Toxicological Chemistry. During his MSc thesis he worked in a forensic laboratory, developing a novel approach to collect VOCs emitted by illegal drugs using Solid Phase Micro-extraction (SPME) technique coupled with Gas chromatography and Mass Spectrometry analysis (GC/MS). Currently he is doing his PhD at Queensland University of Technology. Tommaso's project research is multi-disciplinary where he uses his background in chemistry and toxicological chemistry for analysis in the field of air quality. He works to develop devices to be mounted onboard UAV for Ultrafine particle monitoring, gas sensing and volatile organic compounds sampling and subsequent analysis.*